Received: 12 January 2017 | Revised: 16 March 2017 | Accepted: 25 March 2017

DOI: 10.1002/aoc.3852

FULL PAPER

WILEY Applied Organometallic Chemistry

Acridine-containing Ru^{II}, Os^{II}, Rh^{III} and Ir^{III} Half-Sandwich Complexes: Synthesis, Structure and Antiproliferative Activity

Asanda C. Matsheku[1] | Marian Y.-H. Chen[2] | Sandra Jordaan[3] | Sharon Prince[3] | Gregory S. Smith[2] | Banothile C.E. Makhubela[1]

[1] Department of Chemistry, University of Johannesburg, PO Box 524, Auckland Park, 2006, South Africa

[2] Department of Chemistry, University of Cape Town, Rondebosch 7701, Cape Town, South Africa

[3] Department of Human Biology, Division of Cell Biology, University of the Cape Town, Cape Town, South Africa

Correspondence
Banothile C.E. Makhubela, Department of Chemistry, University of Johannesburg, PO Box 524, Auckland Park, 2006, South Africa.
Email: bmakhubela@uj.ac.za

Funding information
National Research Foundation of South Africa, Grant/Award Number: 95517

Research aimed at enhancing the efficacy of organometallic complexes against cancer, has shown that attaching bio-active molecules to (metallo)drugs often enhances their biological properties. New salicylaldimine and 2-pyridylimine ligands (**L2** and **L3**), containing a bio-active acridine scaffold, were synthesized and complexed to Rh(III), Ir(III), Ru(II) and Os(II) metal ion centers. The resulting acridine-containing half-sandwich complexes have been characterized fully by elemental analysis, FT-IR and NMR spectroscopy, HR-ESI mass spectrometry as well as single crystal X-ray diffraction, for the Rh(III) N^N bidentate complex [RhCp*Cl(**L3**)][BPh_4]. The antiproliferative activity of the ligands (**L2** and **L3**) and complexes (**C1** to **C9**) were evaluated *in vitro* against human promyelocytic leukemia cells (HL60) and normal skin fibroblast cells (FG0). The compounds exhibit good activities against HL60 cells and are consistently selective towards cancerous cells over non-tumorous cells. This study demonstrates the potential of such hybrid compounds to target cancer cells specifically. The most active complex, [RhCp*Cl(**L2**)], exhibited binding to DNA model guanosine-5'-monophosphate (5'-GMP) which suggests a mode of action involving interaction of the complex with 5'-GMP found on DNA backbone.

KEYWORDS
anticancer agents, acridine derivatives, antiproliferative activity, bioorganometallic chemistry, half-sandwich complexes

1 | INTRODUCTION

Cancer formation results from the abnormal growth of cells and their ability to divide in an uncontrolled fashion. Cancer has become the main cause of mortality and there is an urgent need for more effective anticancer drugs.[1,2] Rosenberg's discovery of the anticancer properties of cisplatin (*cis*-diamminedichloroplatinum(II)) was followed by the approval of the first metallodrug, for the treatment of cancer, by the US Food and Drug Administration (FDA) in 1978.[3] Today, cisplatin is one of the most widely used therapeutic metallodrugs and is mostly used as a single agent or in combination with other anticancer agents to treat advanced bladder, testicular and ovarian cancer.[4] However, there are drawbacks associated with the clinical use of cisplatin (and I closely related oxaliplatin and carboplatin) and these include unpleasant side effects, due to toxicity, acquired and intrinsic drug resistance as well as a limited broad spectrum cancer toxicity. This has led to increased efforts directed towards discovering new metal-based anticancer agents.[4–11] To this end, ruthenium, osmium, iridium and rhodium complexes have been investigated and found to exhibit promising cytotoxicity against an array of cancers (Figure 1).[12–20]

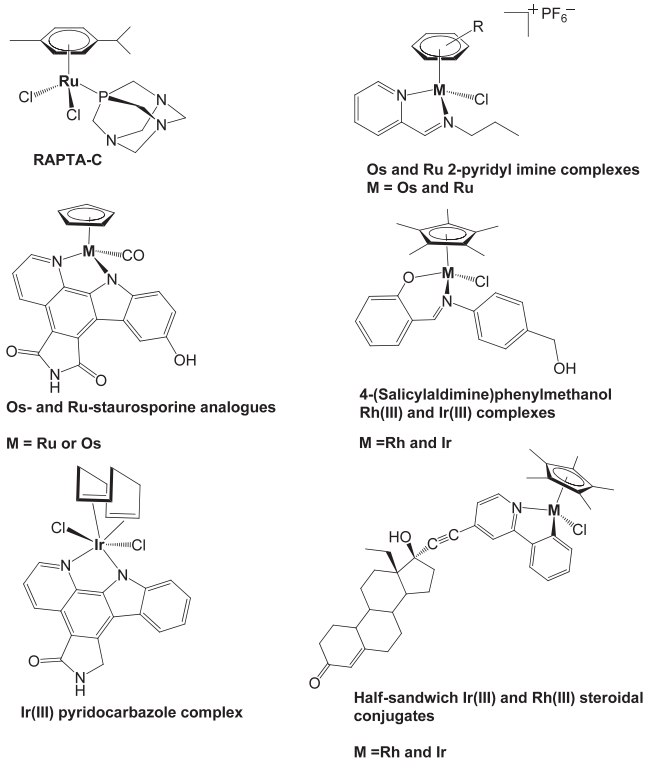

FIGURE 1 Selected structures of Ru(II), Os(II), Rh(III) and Ir(III) complexes that have demonstrated anticancer activity [12–20]

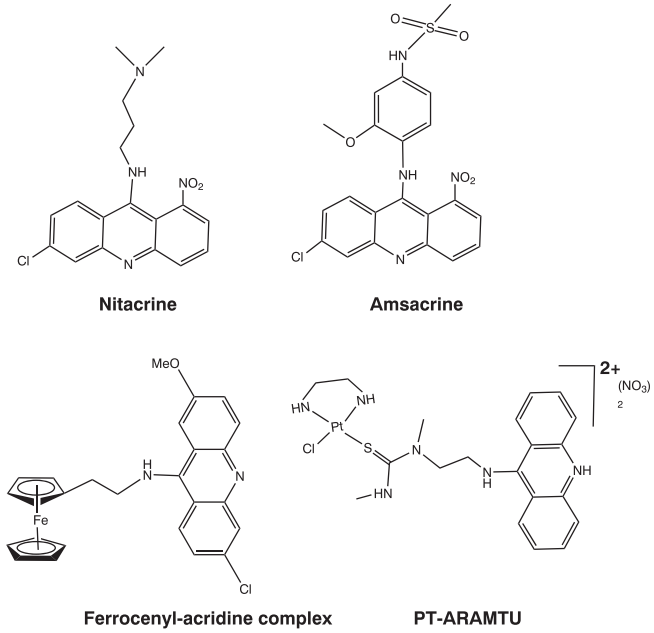

FIGURE 2 Acridine-containing anticancer agents [26,27]

In particular, two ruthenium complexes, KP1339[21] (H_2Na[*trans*-$RuCl_4$(DMSO)(Hind)$_2$] where Hind = indazole) and NAMI-A[22] (H_2Im[*trans*-$RuCl_4$(DMSO)(Him)] where Him = imidazole), have been found to perform exceptionally and are currently undergoing clinical trials.

An approach aimed at enhancing the efficacy of organometallic complexes against cancer, involves coupling the complexes with a compound known to have biological activity.[19,23–25] The biological and chemical stability of acridine and its ability to intercalate DNA has rendered this class of compound useful in the development of targeted anticancer agents. Examples of acridine-bearing anticancer agents are Amsacrine and Nitracrine (Figure 2).

A combination of Amsacrine, Etoposide and Methylprednisolone is used to treat acute lymphoblastic leukemia.[26a–b] Nitracrine has been used to combat various carcinomas such as breast and lung cancer. However, it has been discontinued from further clinical application due to its severe side effects.[26c–d]

Organic intercalators such as acridine can be conjugated to bioactive complexes to afford so-called metallointercalators. Ong *et al*. reported that a ferrocenyl-acridine conjugated complex (Figure 2) displayed high toxicity *in vitro* as compared to a phenyl-derived ferrocene complex, and that the inability of the phenyl-ferrocene complex to intercalate DNA resulted in its low cytotoxic activity.[27a] PT-ACRAMTU (Figure 2) has exhibited promising anticancer results against leukemia and ovarian cancer cell lines and has been demonstrated to be superior to cisplatin.[27b] Several other studies have shown that acridine-containing metallointercalators exhibit enhanced cytotoxicity by a unified dual action involving increased DNA affinity, which is driven by the acridine's intercalating ability, and subsequent DNA damage by the vicinal metal through metal-DNA base pair adduct formation.[28–32]

While examples of Pt, Au and Fe complexes conjugated to acridine moieties are known,[27–33] there remains an opportunity to explore the chemical and anticancer properties of other metal complexes conjugated to acridine. Herein, we report the synthesis and characterization of a series of new 6,9-dichloro-2-methoxyacridine-containing ruthenium(II), osmium(II), rhodium(III) and iridium(III) half-sandwich and ferrocenyl complexes. In the former, the metal ions are coordinated to N^N and N^O bidentate imine ligands. The antiproliferative activity of the complexes against the human promyelocytic leukemia cancer cell line (HL60), and against a normal fibroblast cell line (FG0) were evaluated *in vitro*.

2 | EXPERIMENTAL

2.1 | General considerations

1,2,3,4,5-Pentamethylcyclopentadiene, α-phellandrene, 2-pyridine carboxaldehyde, salicylaldehyde, ethylene diamine, sodium hydride and 9,6-dichloro-2-methoxy

acridine, were all purchased from Sigma Aldrich and used as received. $RuCl_3{\cdot}3H_2O$, $RhCl_3{\cdot}3H_2O$, $IrCl_3{\cdot}3H_2O$ and $K_2OsO_2(OH)_4$ were purchased from Heraeus South Africa. All solvents were of analytical grade and were dried using MBRAUN SPS-800 solvent drying system prior to use. All reactions were carried out in air unless otherwise stated. The precursors, $Ru(p\text{-cym})Cl_2]_2$,[34] $[Os(p\text{-cym})Cl_2]_2$,[35] $[RhCp^*Cl_2]_2$,[36] $[IrCp^*Cl_2]_2$[36] and N^1-(6-chloro-2-methoxyacridin-9-yl)ethane-1,2-diamine (**L1**),[37] were synthesized using literature methods. ^1H NMR, $^{13}C\{^1H\}$ NMR and $^{31}P\{^1H\}$ NMR spectra were recorded on a Bruker Ultrashield 400 (^1H NMR 400.17 MHz, $^{13}C\{^1H\}$ NMR 101.02 MHz and $^{13}P\{^1H\}$ NMR 161.99 MHz) spectrometer and chemical shifts are reported using tetramethylsilane and H_3PO_4 (for $^{31}P\{^1H\}$ NMR) spectra as the internal standard. Fourier transform infrared (IR) spectra were obtained using the Perkin Elmer Spectrum 100 FT-IR spectrometer with an attenuated total reflection (ATR) accessory. High resolution (HR) ESI-mass spectrometry was obtained using Waters API Quattro Micro triple quadrupole mass spectrometer in the positive ion mode. Where the ESI probe was injected into a stream of methanol at a cone voltage of 15 eV. Melting points were determined using a Buchi B-540 apparatus and elemental analyses were performed on a Thermo Scientific FLASH 2000 CHNS-O analyzer.

2.2 | Synthesis of 2-(((2-((6-Chloro-2-methoxyacridin-9-yl)amino)ethyl)imino)methyl) phenol (L2)

Salicylaldehyde (0.142 g, 1.163 mmol) in dichloromethane (20 ml) was added dropwise to a solution of **L1** (0.350 g, 1.166 mmol) in dichloromethane (20 ml). Anhydrous sodium sulfate (approximately 2.00 g) was added to this mixture, in order to 'mop-up' the water by-product in the Schiff base condensation reaction and drive the reaction forward. This reaction mixture was allowed to stir at room temperature for 48 hours. After 48 hours, the sodium sulfate was removed by filtration. The filtrate was transferred to a separating funnel and washed with water (3 × 40 ml). Finally, the organic layer was dried using anhydrous sodium sulfate. The sodium sulfate was then filtered, and the solvent was removed from the filtrate by rotary evaporation to afford **L2**, as an orange crystalline solid. (0.337 g, 72% yield). Melting point: 141–143°C. Elemental Analysis, Calc. for $C_{23}H_{20}ClN_3O_2$: C 68.11, H 4.97, N 10.30 %; Found: C 68.34, H 4.79, N 9.98 %. ^1H NMR (400 MHz, DMSO-d_6): δ(ppm) = 3.71 (t, J = 12 Hz, 2H, CH_2); 3.77 (s, 3H, O*Me*); 3.87 (br s, 2H, CH_2); 4.10 (br s, 1H, N*H*); 6.82 (t, J = 15 Hz, 1H, *Ar*); 6.96 (d, J = 9 Hz, 1H, *Ar*); 7.05 (d, J = 2.4 Hz, 1H, *Ar*); 7.08 (d, J = 1.6 Hz, 1H, $Ar_{acridine}$); 7.24 (d, J = 6 Hz, 1H, $Ar_{acridine}$); 7.31-7.42 (m, 2H, *Ar* and $Ar_{acridine}$); 7.95-8.01 (m, 2H, $Ar_{acridine}$); 8.26 (s, 1H, *H*C=N); 8.37 (br s, 1H, $Ar_{acridine}$);12.90 (br s, 1H, O*H*). $^{13}C\{^1H\}$ NMR (101 MHz, DMSO-d_6): δ (ppm) = 49.9 (CH_2); 54.9 (O*Me*); 59.5 (CH_2); 97.7 (*Ar*); 116.6 (*Ar*); 118.1 ($Ar_{acridine}$); 118.6 (*Ar*); 118.8 ($Ar_{acridine}$); 123.6-124.2 ($Ar_{acridine}$); 124.7 ($Ar_{acridine}$); 124.8 (*Ar*); 128.1 ($Ar_{acridine}$); 131.2 ($Ar_{acridine}$); 131.3(*Ar*); 132.5 ($Ar_{acridine}$); 134.4 ($Ar_{acridine}$); 146.5 ($Ar_{acridine}$); 147.8 ($Ar_{acridine}$); 148.1 ($Ar_{acridine}$); 156.2 ($Ar_{acridine}$); 160.5 (*Ar*); 167.3 (H*C*=N). FT-IR (ATR): ν(cm^{-1}) = 3555 (O-H); 3353 (N-H); 1630 $(C{=}N)_{imine}$, 1607 $(C{=}N)_{acr.\ imine}$. HR-ESI-MS (+): Calc. for $C_{23}H_{20}ClN_3O_2$ $[M]^+$ m/z = 405.1244; Found: m/z = 406.1240 $[M+H]^+$.

2.3 | Synthesis of N^1-(6-Chloro-2-methoxyacridin-9-yl)-N^2-(pyridin-2-ylmethylene)ethane-1,2-diamine (L3)

2-Pyridinecarboxaldehyde (0.330 g, 3.083 mmol) in dichloromethane (20 ml) was added dropwise to a solution of **L1** (0.928 g, 3.083 mmol) dissolved in dichloromethane (20 ml). Anhydrous sodium sulfate (approximately 2.00 g) was added to this mixture, in order to 'mop-up' the water by-product in the Schiff-base condensation reaction and drive the reaction forward. This reaction mixture was allowed to stir at room temperature for 48 hours. After 48 hours, sodium sulfate was removed by filtration. The filtrate was transferred to a separating funnel and washed with water (3 × 40 ml). The collected organic layer was then dried with anhydrous sodium sulfate. The sodium sulfate was then filtered and the solvent was removed from the filtrate by rotary evaporation to afford **L3** as an orange solid (0.901 g, 75% yield). Melting point: 108–110°C. Elemental Analysis, Calc. for $C_{22}H_{19}ClN_4O$: C 67.70, H 4.90, N 14.30% Found: C 67.42, H 4.66, N 14.41 %. ^1H NMR (400 MHz, DMSO-d_6): δ (ppm) = 3.90 (s, 3H, O*Me*); 3.97 (t, J = 8.0 Hz, 2H, CH_2); 4.05 (t, J = 8.0 Hz, 2H, CH_2); 5.41 (br s, 1H, N*H*); 7.18 (d, J = 4 Hz, 1H, $Ar_{acridine}$); 7.29 (d, J = 4 Hz, 1H, $Ar_{acridine}$); 7.35 – 7.41 (m, 1H, $Ar_{acridine}$); 7.76 (t, J = 16 Hz, 1H, *Ar*); 7.94-7.98 (m, , 2H, *Ar*); 8.00- 8.07 (m, 2H, $Ar_{acridine}$); 8.42 (s, 1H, *H*C=N); 8.45 (s, 1H, $Ar_{acridine}$); 8.67 (d, J = 8.0 Hz, 1H, *Ar*). $^{13}C\ \{^1H\}$ NMR (101 MHz, DMSO-d_6): δ (ppm) = 51.0 (CH_2); 55.4 (O*Me*); 61.1 (CH_2); 99.0 (*Ar*); 116.9 (*Ar*); 119.0 ($Ar_{acridine}$); 121.3 (*Ar*); 124.3 ($Ar_{acridine}$); 124.8 ($Ar_{acridine}$); 124.9 ($Ar_{acridine}$); 125.1 (*Ar*); 128.4 ($Ar_{acridine}$); 131.6 ($Ar_{acridine}$); 134.7 (*Ar*); 136.6 ($Ar_{acridine}$); 138.3 ($Ar_{acridine}$); 148.4 ($Ar_{acridine}$); 149.6 ($Ar_{acridine}$); 149.7 ($Ar_{acridine}$); 156.3 ($Ar_{acridine}$); 164.2 (H*C*=N). FT-IR (ATR): ν (cm^{-1}) = 3357 (N-H); 1647, $(C{=}N)_{imine}$ 1605 $(C{=}N)_{acr.\ imine}$, 1597 $(C{=}N)_{pyridylimine}$. HR-ESI-MS (+): Calc. for $C_{22}H_{19}ClN_4O$ $[M]^+$ m/z = 390.1247 Found: m/z = 391.1253 $[M+H]^+$.

2.4 | Synthesis of C1

L1 (0.202 g, 0.671 mmol) was dissolved in 15 mL EtOH. Ferrocenylcarboxaldehyde (0.170 g, 0.791 mmol) was dissolved in 15 ml EtOH and added drop-wise to the **L1** solution. Molecular sieves (4 Å, 2.00 g) were added. The reaction mixture was left to stir for 28 hours and followed by refluxing at 80°C for 20 hours. The molecular sieves were filtered off and the resulting solution was reduced to a third of its original volume by rotary evaporation. The solution was added drop-wise to cold petroleum ether (100 ml) and a red solid precipitated out. This red solid was collected by gravity filtration and was later found to be ferrocene carboxaldehyde. The filtrate was left at -2°C overnight (± 18 hours) during which time **C1** precipitated from solution as an orange solid. **C1** was collected by filtration (suction) and dried under vacuum for 8 hours. (0.131 g, 39 % yield). Melting point: 63-65°C. Elemental Analysis, Calc. for $C_{27}H_{24}ClFeN_3O$: C 65.15, H 4.86, N 8.44% Found: C 65.43, H 4.83, N 8.60%. ^{1}H NMR (400 MHz, DMSO-d_6): δ (ppm) = 3.76 (t, J = 5.5 Hz, 2H, CH_2); 3.90 - 4.04 (m, 10H, *H*-Cp, O*Me*, CH_2); 4.33 (br s, 2H, *H*-Cp); 4.50 (br s, 2H, *H*-Cp); 6.77 - 6.86 (br s, 1 H, N*H*); 7.30 - 7.46 (m, 2H, $Ar_{acridine}$); 7.70 (d, J = 1.7 Hz, 1H, $Ar_{acridine}$); 7.80 - 7.92 (m, 2H, $Ar_{acridine}$); 8.13 (s, 1H, *H*C=N); 8.51 (d, J = 9.2 Hz, 1H, $Ar_{acridine}$). ^{13}C{^{1}H} NMR (101 MHz, DMSO-d_6): δ (ppm) = 50.6 (*C*H$_2$); 56.2 (O*Me*); 61.6 (*C*H$_2$); 68.6 (Cp) 69.2 (Cp); 70.5 (Cp); 81.0 ($Ar_{acridine}$); 115.2 ($Ar_{acridine}$); 117.8 ($Ar_{acridine}$); 123.2 ($Ar_{acridine}$); 124.7 ($Ar_{acridine}$); 127.3 ($Ar_{acridine}$); 127.7 ($Ar_{acridine}$); 131.3 ($Ar_{acridine}$); 133.9 ($Ar_{acridine}$); 136.6 ($Ar_{acridine}$); 148.3 ($Ar_{acridine}$); 151.2-153.2 ($Ar_{acridine}$); 155.5 ($Ar_{acridine}$); 162.5 (H*C*=N). FT-IR (ATR): ν (cm^{-1}) = 3425 (N-H); 1630, (C=N) $_{imine}$; 1606 (C=N)$_{acr.\ imine}$. HR-ESI-MS (+): Calc. for $C_{27}H_{24}ClFeN_3O$ $[M]^+$ m/z = 497.0957 Found: m/z = 498.1036 $[M+H]^+$.

2.5 | Synthesis of [RhCp*Cl(L2)] (C2)

To a stirring solution of **L2** (0.100 g, 0.246 mmol) in dichloromethane (40 ml), Sodium hydride (0.00590 g, 0.246 mmol) was added and the mixture was allowed to stir at room temperature for 15 minutes. After 15 minutes, $[RhCl_2Cp^*]_2$ (0.0759 g, 0.123 mmol) in dichloromethane (20 ml) was added and this solution was allowed to continue stirring at room temperature for 24 hours. After 24 hours, the reaction mixture was filtered by gravity to remove any unreacted material. The filtrate was then reduced (to ≈ 5 ml) and cold diethyl ether (20 ml) was added drop-wise to the solution to precipitate **C2**. **C2** was then collected by suction filtration as an orange solid and dried under vacuum for 3 hours. (0.082 g, 98 % yield). Melting point: 149–151°C. Elemental Analysis, Calc. for $C_{33}H_{34}Cl_2N_3O_2Rh$: C 58.42, H 5.05, N 6.19% Found: C 58.70, H 5.08, N 5.97 %. ^{1}H NMR (400 MHz, DMSO-d_6): δ (ppm) = 1.64 (s, 15 H, *Me*-Cp*); 3.65 (s, 3 H, O*Me*); 3.98 (br, s 2H, CH_2); 4.18 (br, s 1H, CH_2); 4.33 (br, s, 1H, CH_2); 6.30 (t, J = 8 Hz, 1H, *Ar*); 6.64-6.88 (m, , 2H, *Ar*); 7.05-7.37 (m, 4H, *Ar* and $Ar_{acridine}$); 7.68-7.81 (m, 2H, $Ar_{acridine}$); 7.98 (s, 1 H, *H*C=N); 8.14 (d, J = 9 Hz, 1H, $Ar_{acridine}$). ^{13}C{^{1}H} NMR (101 MHz, DMSO-d_6): δ (ppm) = 9.06 (*Me*- Cp*); 48.2 (*C*H$_2$); 56.4 (O*Me*); 65.9 (*C*H$_2$); 93.6 (Cp*); 93.8 (*Ar*); 113.0 (*Ar*); 114.04 ($Ar_{acridine}$); 117.6 (*Ar*); 119.3 ($Ar_{acridine}$); 123.3 ($Ar_{acridine}$); 124.3 ($Ar_{acridine}$); 125.1 (*Ar*); 125.9 ($Ar_{acridine}$); 126.0 ($Ar_{acridine}$); 131.6 (*Ar*); 134.9 ($Ar_{acridine}$); 135.3 ($Ar_{acridine}$); 136.2 ($Ar_{acridine}$); 150.7 ($Ar_{acridine}$); 152.3-153.1 ($Ar_{acridine}$); 156.5 ($Ar_{acridine}$) 161.9 (*Ar*); 166.8 (H*C*=N). FT-IR (ATR): ν (cm^{-1}) = 3309 (N-H), 1616 (C=N)$_{imine}$, 1605 (C=N)$_{acr.\ imine}$. HR-ESI-MS (+): Calc. for $C_{33}H_{34}Cl_2N_3O_2Rh$ $[M]^+$ m/z = 677.1083 Found: m/z = 678.1156 $[M+H]^+$, m/z = 642.1393 $[M-Cl]^+$.

Complexes **C3**-**C5** were prepared following the same procedure as described for **C2**, using the appropriate reagents.

2.6 | Synthesis of [IrCp*Cl(L2)] (C3)

Sodium hydride (0.00590 g, 0.246 mmol) was added to a stirring solution of **L2** (0.100 g, 0.246 mmol). After 15 minutes, $[IrCl_2Cp^*]_2$ (0.0981 g, 0.123 mmol) was added and this solution was allowed to continue stirring at room temperature for 24 hours. **C3** was isolated as a mustard yellow solid (0.081 g, 86% yield). Melting point: 219–223°C. Elemental Analysis, Calc. for $C_{33}H_{34}Cl_2N_3O_2Ir$: C 51.62, H 4.46, N 5.47 % Found: C 51.20, H 4.67, N 5.72 ^{1}H NMR (400 MHz, DMSO-d_6): δ (ppm) = 1.49 (s, 15 H, *Me*-Cp*); 3.71 (s, 3H, O*Me*); 4.07 (br s, 2H, CH_2); 4.38 (br s, 1H, CH_2); 4.52 (s, 1H, CH_2); 6.30 (t, J = 6.9 Hz, 1H, *Ar*); 6.65 (d, 1H, *Ar*); 6.83 (d, J = 6.7 Hz, 1H, *Ar*); 7.19-7.30 (m, 1H, $Ar_{acridine}$); 7.45 (d, J = 8.8 Hz,1H, $Ar_{acridine}$); 7.53 (d, J = 8.4 Hz, 1H, *Ar*); 7.70 (s, 1H, $Ar_{acridine}$); 7.85 (d, J = 8.7 Hz, 1H, $Ar_{acridine}$); 7.95 (s, 1H, $Ar_{acridine}$); 8.04 (s, 1H, *H*C=N); 8.52 (d, J = 8.8 Hz, 1H, $Ar_{acridine}$). ^{13}C{^{1}H} NMR (101 MHz, DMSO-d_6): δ (ppm) = 9.16 (*Me*-Cp*); 48.4 (*C*H$_2$); 56.3 (O*Me*); 68.6 (*C*H$_2$); 95.8 (Cp*); 99.8 (*Ar*); 110.3 (*Ar*); 114.3 ($Ar_{acridine}$); 115.1 (*Ar*); 118.1 ($Ar_{acridine}$); 122.4 ($Ar_{acridine}$); 125.3 ($Ar_{acridine}$); 126.1 (*Ar*); 126.5 ($Ar_{acridine}$); 127.8 ($Ar_{acridine}$); 130.8 (*Ar*); 134.3 ($Ar_{acridine}$); 135.2 ($Ar_{acridine}$); 136.1 ($Ar_{acridine}$); 150.2 ($Ar_{acridine}$); 151.7 ($Ar_{acridine}$) 152.1 ($Ar_{acridine}$); 156.6 ($Ar_{acridine}$); 163.4 (*Ar*); 165.3; (H*C*=N). FT-IR (ATR): ν (cm^{-1}) = 3321 (N-H); 1617 (C=N)$_{imine}$, 1602 (C=N)$_{acr.\ imine}$. %. HR-ESI-MS (+): Calc. for $C_{33}H_{34}Cl_2N_3O_2Ir$ $[M]^+$ m/z = 767.1657 Found: m/z = 768.1721 $[M+H]^+$, m/z = 632.1963 $[M-Cl]^+$.

2.7 | Synthesis of [Ru(*p*-cym)Cl(L2)] (C4)

L2 (0.0800 g, 0.197 mmol) and sodium hydride (0.00437 g, 0.197 mmol) were allowed to stir at room temperature for 15 minutes. After 15 minutes, $[Ru(p\text{-cym})Cl_2]_2$ (0.0603 g, 0.0985 mmol) was added and this solution was allowed to continue stirring at room temperature for 24 hours. **C4** was isolated as an orange solid (0.0484 g, 73% yield). Melting point: 217–219°C. Elemental Analysis, Calc. for $C_{33}H_{33}Cl_2N_3O_2Ru$: C 58.67, H 4.92, N 6.22% Found: C 58.80, H 4.99, N 5.99%. ^{1}H NMR (400 MHz, DMSO-d_6): δ (ppm) = 1.03, 1.17 (d, J = 6.6 Hz, 6H, *p*-cym$_{CH3}$); 2.11 (s, 3H, *p*-cym$_{CH3}$); 2.64 (m, 1H, *p*-cym$_{CH}$); 3.57 (s, 3H, O*Me*); 4.19 (br s, 2H, CH_2); 4.48 (br s, 1H, CH_2); 4.74 (br s, 1H, CH_2); 5.36-5.79 (m, 4H, *p*-cym$_{Ar}$); 6.20 (t, J = 7.0 Hz, 1H, *Ar*); 6.49 (s, 1H, *Ar*); 6.65 (d, J = 8.4 Hz, 1H, *Ar*); 7.01-7.15 (m, 1H, *Ar*$_{acridine}$); 7.31-7.43 (m, 3H, *Ar* and *Ar*$_{acridine}$); 7.63 (s, 1H, *Ar*$_{acridine}$); 7.81 (d, J = 9.1 Hz, *Ar*$_{acridine}$); 7.92 (s, 1H, *H*C=N); 8.38 (d, J = 9.1 Hz, 1H, *Ar*$_{acridine}$). ^{13}C{^{1}H} NMR (101 MHz, DMSO-d_6): δ (ppm) = 18.0, 19.2 (*p*-cym$_{CH3}$); 21.6 (*p*-cym$_{CH3}$); 32.0 (*p*-cym$_{CH}$); 48.3 (*C*H$_2$); 56.0 (O*Me*); 69.9 (*C*H$_2$); 77.3-98.5 (*p*-cym$_{Ar}$); 99.8 (*Ar*); 111.2 (*Ar*); 114.4 (*Ar*$_{acridine}$); 116.2 (*Ar*); 117.6 (*Ar*$_{acridine}$); 121.8 (*Ar*$_{acridine}$); 124.0 (*Ar*$_{acridine}$); 125.8 (*Ar*); 126.3 (*Ar*$_{acridine}$); 131.3 (*Ar*); 134.9 (*Ar*$_{acridine}$); 135.5 (*Ar*$_{acridine}$) 135.7 (*Ar*$_{acridine}$); 149.8 (*Ar*$_{acridine}$), 151.4 (*Ar*$_{acridine}$); 152.7-153.4 (*Ar*$_{acridine}$), 156.7 (*Ar*$_{acridine}$); 164.4 (*Ar*); 166.3 (H*C*=N). FT-IR (ATR): ν (cm^{-1}) = 3337 (N-H); 1618, (C=N)$_{imine}$ 1606 (C=N)$_{acr.\ imine}$. HR-ESI-MS (+): Calc. for $C_{33}H_{33}Cl_2N_3O_2Ru$ $[M]^+$ m/z = 675.0993 Found: m/z = 676.1064 $[M+H]^+$, m/z = 640.1305 $[M\text{-}Cl]^+$.

2.8 | Synthesis of [Os(*p*-cym)Cl(L2)] (C5)

L2 (0.150 g, 0.370 mmol) and sodium hydride (0.0088 g, 0.370 mmol) were allowed to stir at room temperature for 15 minutes. After 15 minutes, $[Os(p\text{-cym})Cl_2]_2$ (0.146 g, 0.185 mmol) was added and this mixture was allowed to continue stirring at room temperature for 24 hours. **C5** was isolated as an orange solid (0.0826 g, 58% yield). Melting point: 125128°C. Elemental Analysis, Calc. for $C_{33}H_{33}Cl_2N_3O_2Os$: C 51.83, H 4.35, N 5.49 % Found: C 51.98, H 4.76, N 5.04 %. ^{1}H NMR (400 MHz, DMSO-d_6): δ (ppm) = 1.02, 1.16 (d, J = 6.7 Hz, 6H, *p*-cym$_{CH3}$); 2.13 (s, 3H, *p*-cym$_{CH3}$); 2.59 (m, 1H, *p*-cym$_{CH}$); 3.64 (s, 3H, O*Me*); 4.07 (br s, 2H, CH_2); 4.38 (br s, 1H, CH_2); 4.63 (br. s, 1H, CH_2); 5.71-6.15 (m, , 4H, *p*-cym$_{Ar}$); 6.30 (t, J = 7.3 Hz, 1H, *Ar*); 6.62 (d, J = 8.3 Hz, 1H, *Ar*); 6.79 (m, 1H, *Ar*); 7.10-7.24 (m, 2H, *Ar*$_{acridine}$); 7.43-7.79 m, 4H, *Ar* and *Ar*$_{acridine}$); 7.90 (s, 1H, *H*C=N); 8.41 (d, J = 9.1 Hz, 1H, *Ar*$_{acridine}$). ^{13}C{^{1}H} NMR (101 MHz, DMSO-d_6): δ (ppm) = 18.7, 19.6 (*p*-cym$_{CH3}$); 22.4 (*p*-cym$_{CH3}$); 31.1 (*p*-cym$_{CH}$); 49.1 (*C*H$_2$); 55.8 (O*Me*); 65.4 (*C*H$_2$); 76.4-99.6 (*p*-cym$_{Ar}$); 100.2 (*Ar*); 110.7 (*Ar*); 113.8 (*Ar*$_{acridine}$); 115.6 (*Ar*); 118.1 (*Ar*$_{acridine}$); 120.9 (*Ar*$_{acridine}$); 124.3 (*Ar*$_{acridine}$); 125.9 (*Ar*); 126.6 (*Ar*$_{acridine}$); 131.9 (*Ar*); 133.8 (*Ar*$_{acridine}$); 134.7 (*Ar*$_{acridine}$) 135.3 (*Ar*$_{acridine}$); 150.2 (*Ar*$_{acridine}$), 151.5 (*Ar*$_{acridine}$); 152.6-153.0 (*Ar*$_{acridine}$), 157.1 (*Ar*$_{acridine}$); 163.8 (*Ar*); 166.4 (H*C*=N). FT-IR (ATR): ν (cm^{-1}) = 3313 (N-H); 1615, (C=N)$_{imine}$ 1604 (C=N)$_{acr.\ imine}$. HR-ESI-MS (+): Calc. for $C_{33}H_{33}Cl_2N_3O_2Os$ $[M]^+$ m/z = 765.1565 Found: m/z = 766.1574 $[M+H]^+$, m/z = 730.1816 $[M\text{-}Cl]^+$.

2.9 | Synthesis of [RhCp*Cl(L3)][BPh$_4$] (C6)

To a stirring solution of **L3** (0.100 g, 0.256 mmol) in chloroform (20 ml), $[RhCl_2Cp^*]_2$ (0.083 g, 0.128 mmol) in chloroform (20 ml) was added. This solution was allowed to stir at room temperature for 24 hours. After 24 hours, the solvent was removed by rotary evaporation. The remaining solid was dissolved in methanol (15 ml) and sodium tetraphenylborate (0.0439 g, 0.128 mmol) was added, and the mixture was allowed to stir at room temperature for 30 minutes. After 30 minutes, a precipitate formed which was collected by filtration and washed with methanol (3 x 20 ml) to afford **C6** (0.0797 g, 63% yield) as a dark mustard solid (which was dried under vacuum for 2 hours). Melting point: 178–180°C. Elemental Analysis, Calc. for $C_{56}H_{54}BCl_2N_4ORh$: C 68.38, H 5.53, N 5.70% Found: C 68.80, H 5.66, N 5.66 %. ^{1}H NMR (400 MHz, DMSO-d_6): δ (ppm) = 1.65 (s, 15H, *Me*-Cp*); 3.50 (s, 3H, O*Me*); 3.98 - 4.23 (m, 2H, CH_2), 4.45 (br s, 1H, CH_2), 4.54 (br s, 1H, CH_2); 6.22 (br s, 1H, N*H*), 6.70 - 6.86 (m, 4H, B*Ph*$_4^-$); 6.93-7.25 (m, 17H, B*Ph*$_4^-$ and *Ar*); 7.39 (t, J = 10 Hz, 1H, *Ar*); 7.81 - 8.05 (m, 4H, *Ar* and *Ar*$_{acridine}$); 8.21 - 8.41 (m, 2H, *Ar*$_{acridine}$); 8.36 (br s, 1H, *H*C=N); 8.48 (s, 1H, *Ar*$_{acridine}$); 9.05 (s, J = 5.0 Hz, 1H, *Ar*). ^{13}C{^{1}H} NMR (101 MHz, DMSO-d_6): δ (ppm) = 8.69 (*Me*-Cp*); 47.6 (*C*H$_2$); 55.7 (O*Me*); 61.8 (*C*H$_2$); 97.5 (Cp*); 99.5 (*Ar*); 112.6 (*Ar*); 120.4 (*Ar*$_{acridine}$); 121.6 (*Ar*); 123.8 (*Ar*$_{acridine}$); 125.4 (*Ar*$_{acridine}$); 126.1 (*Ar*$_{acridine}$); 128.9 (*Ar*$_{acridine}$); 129.6 (*Ar*$_{acridine}$); 130.0 (*Ar*$_{acridine}$); 135.6 (*Ar*); 136.8 (*Ar*$_{acridine}$); 140.6 (*Ar*$_{acridine}$); 145.2 9 (*Ar*); 151.7 (*Ar*$_{acridine}$); 152.3-152.9 (*Ar*$_{acridine}$); 155.7 (*Ar*$_{acridine}$); 169.7 (H*C*=N). FT-IR (ATR): ν (cm^{-1}) = 3329 (N-H); 1630 (C=N)$_{imine}$, 1604 (C=N) $_{acr.\ imine}$, 1600 (C=N)$_{pyridylimine}$. HR-ESI-MS (+): Calc. for $C_{32}H_{34}Cl_2N_4ORh$ $[M]^+$ m/z = 663.1165 Found: m/z = 983.2942 $[(M+H)^{2+}BPh_4^-]$ $^+$, m/z = 663.1174 $[M]^+$.

Complexes **C7**-**C9** were prepared following the same procedure as described for **C6**, using the appropriate reagents. For **C8** and **C9**, the reaction was stirred at room temperature for 1.5 hours in the first step.

2.10 | Synthesis of [IrCp*Cl(L3)][BPh_4] (C7)

L3 (0.096 g, 0.246 mmol) in chloroform (40 ml) and $[IrCl_2Cp^*]_2$ (0.102 g, 0.123 mmol) were used. After 24 hours of stirring at room temperature, the solvent was removed by rotary evaporation. The remaining solid was dissolved in methanol (15 ml) and sodium tetraphenylborate (0.042 g, 0.123 mmol) was added. The product (**C7**) precipitated out as a dark orange solid. (0.095 g, 72 % yield). Melting point: 189–191°C. Elemental Analysis, Calc. for $C_{56}H_{54}BCl_2N_4OIr$: C 62.68, H 5.07, N 5.22 % Found: C 62.70, H 5.14, N 5.46 %. ^{1}H NMR (400 MHz, DMSO-d_6): δ(ppm) = 1.65 (s, 15H, *Me*-Cp*); 3.60 (s, 3H, O*Me*); 4.06 (br s, 2H, CH_2), 4.35 - 4.67 (m, 2H, CH_2); 6.27 (br s, 1H, N*H*); 6.73 - 6.82 (m, 4H, BPh_4^-); 6.89-7.19 (m, 16H, BPh_4^-); 7.42-7.55 (m, 2H, *Ar*); 7.76 - 8.06 (m, 4H, *Ar* and $Ar_{acridine}$); 8.19 - 8.45 (m, 3H, $Ar_{acridine}$); 8.37 (br s, 1H, *H*C=N); 9.03 (d, J = 5.0 Hz, 1 H, *Ar*). ^{13}C{^{1}H} NMR (101 MHz, DMSO-d_6): δ(ppm) = 7.70 (*Me*-Cp*); 47.2 (*C*H_2); 55.1 (*Me*-Cp* and O*Me*); 62.4 (*C*H_2); 89.4 (Cp*); 99.3 (*Ar*); 111.4 (*Ar*); 117.4 ($Ar_{acridine}$); 121.0 (*Ar*); 123.3 ($Ar_{acridine}$); 124.8 ($Ar_{acridine}$); 128.4 ($Ar_{acridine}$); 129.9 ($Ar_{acridine}$); 130.4 ($Ar_{acridine}$); 131.2 ($Ar_{acridine}$); 135.1 (*Ar*); 138.2 ($Ar_{acridine}$); 140.12 ($Ar_{acridine}$), 146.4 (*Ar*); 152.9 ($Ar_{acridine}$); 154.3-154.8 ($Ar_{acridine}$); 155.2 ($Ar_{acridine}$); 171.1 (H*C*=N). FT-IR (ATR): ν (cm^{-1}) = 3340 (N-H); 1630 (C=N)$_{imine}$, 1606 (C=N)$_{acr.\ imine}$, 1601(C=N)$_{pyridylimine}$. HR-ESI-MS (+): Calc. for $C_{32}H_{34}Cl_2IrN_4O$ $[M]^+$ *m/z* = 753.1739. Found: *m/z* = 1073.3516 $[(M+H)^{2+}BPh_4^-]^+$, *m/z* = 753.1736 $[M]^+$.

2.11 | Synthesis of [Ru(*p*-cym)Cl(L3)][BPh_4] (C8)

L3 (0.124 g, 0.318 mmol) in chloroform (40 ml) and [Ru(*p*-cym)Cl_2]$_2$ (0.0970 g, 0.159 mmol) were used. This solution was allowed to stir at room temperature for 1 hour 30 minutes. After 1 hour 30 minutes, the solvent was removed by rotary evaporation. The remaining solid was dissolved in methanol (15 ml), and sodium tetraphenylborate (0.0544 g, 0.159 mmol) was added. The product (**C8**) precipitated out as an orange solid. (0.097 g, 62 % yield). Melting point: 236–239°C. Elemental Analysis, Calc. for $C_{56}H_{53}BCl_2N_4ORu$: C 68.57, H 5.45, N 5.71 % Found: C 68.20, H 5.17, N 5.47 %. ^{1}H NMR (400 MHz, DMSO-d_6): δ(ppm) = 0.94, 1.00 (d, J = 8.0 Hz, 6H, *p*-cym$_{CH3}$); 2.21 (s, 3H, *p*-cym$_{CH3}$); 2.57 (m, 1H, *p*-cym$_{CH}$); 3.60 (s, 3H, O*Me*); 4.21 (br s, 2H, CH_2); 4.32 (br s, 1H, CH_2); 4.82 (br s, 1H, CH_2); 5.99-6.24 (m, 5H, *Ar* and *p*-cym$_{Ar}$); 6.55 (t, J = 8 Hz, 4H, BPh_4^-); 6.90-7.16 (m, 16H, BPh_4^-); 7.19-7.28 (m, 1H, *Ar*); 7.86-8.01 (m, 4H, $Ar_{acridine}$ and *Ar*); 8.24-8.46 (m, 3H, $Ar_{acridine}$); 8.36 (s, 1H, *H*C=N); 9.04 (d, J = 8 Hz, 1H, *Ar*). ^{13}C{^{1}H} NMR (101 MHz, DMSO-d_6): δ(ppm) = 18.8, 19.9 (*p*-cym$_{CH3}$); 21.7 (*p*-cym$_{CH3}$); 31.0 (*p*-cym$_{CH}$); 49.0 (*C*H_2); 56.1 (O*Me*); 66.9 (*C*H_2); 84.6-101.4 (*p*-cym$_{Ar}$); 103.2 (*Ar*), 105.3 (*Ar*), 109.5 ($Ar_{acridine}$); 115.9 (*Ar*); 118.4 ($Ar_{acridine}$); 122.0 ($Ar_{acridine}$); 125.2 ($Ar_{acridine}$); 126.4 ($Ar_{acridine}$); 131.8 ($Ar_{acridine}$); 134.0 (*Ar*); 136.0 ($Ar_{acridine}$), 137.2 ($Ar_{acridine}$), 147.8 (*Ar*); 150.6 ($Ar_{acridine}$); 151.4-152.8 ($Ar_{acridine}$); 154.4 ($Ar_{acridine}$); 156.2 ($Ar_{acridine}$); 170.4 (*H*C=N). FT-IR (ATR): ν(cm^{-1}) = 3270 (N-H); 1627 (C=N)$_{imine}$, 1605 (C=N)$_{acr.\ imine}$, 1601(C=N)$_{pyridylimine}$. HR-ESI-MS (+): Calc. for $C_{33}H_{36}Cl_2N_4ORu$ $[M]^+$ *m/z* = 661.1075 Found: *m/z* = 981.2861 $[(M+H)^{2+}BPh_4^-]^+$, *m/z* = 661.1077 $[M]^+$.

2.12 | Synthesis of [Os(*p*-cym)Cl(L3)][BPh_4] (C9)

L3 (0.150 g, 0.384 mmol) in chloroform (40 ml) and [Os(*p*-cym)Cl_2]$_2$ (0.0152 g, 0.192 mmol) were used. The solution was stirred at room temperature for 1 hour 30 minutes. After 1 hour 30 minutes, the solvent was removed by rotary evaporation. The remaining solid was dissolved in methanol (15 ml), and sodium tetraphenylborate (0.0657 g, 0.192 mmol) was added. The product (**C7**) precipitated out as a brown solid. (0.125 g, 61 % yield). Melting point: 155–158°C. Elemental Analysis, Calc. for $C_{56}H_{53}BCl_2N_4OOs$: C 62.86, H 4.99, N 5.24 % Found: C 62.37, H 4.85, N 5.27 %. ^{1}H NMR (400 MHz, DMSO-d_6): δ(ppm) = 0.92, 1.08 (d, J = 8 Hz, 6H, *p*-cym$_{CH3}$); 2.19 (s, 3H, *p*-cym$_{CH3}$); 2.63 (m, 1H, *p*-cym$_{CH}$); 3.58 (s, 3H, O*Me*); 4.23 (br s, 2H, CH_2); 4.36 (br s, 1H, CH_2); 4.80 (br s, 1H, CH_2); 5.98-6.19 (m, 5H, *Ar* and *p*-cym$_{Ar}$); 6.42 (t, J = 8 Hz, 4H, BPh_4); 6.94-7.14 (m, 16H, BPh_4^-); 7.17-7.32 (m, 1H, *Ar*); 7.82-8.05 (m, 4H, $Ar_{acridine}$ and *Ar*); 8.19-8.43 (m, 3H, $Ar_{acridine}$); 8.35 (s, 1H, *H*C=N); 9.01 (d, J = 8 Hz, 1H, *Ar*). ^{13}C{^{1}H} NMR (101 MHz, DMSO-d_6): δ(ppm) = 19.1, 20.2 (*p*-cym$_{CH3}$); 22.1 (*p*-cym$_{CH3}$); 31.6 (*p*-cym$_{CH}$); 49.4 (*C*H_2); 57.5 (O*Me*); 67.7 (*C*H_2); 86.2-102.3 (*p*-cym$_{Ar}$); 104.8 (*Ar*), 111.3 (*Ar*), 112.4 ($Ar_{acridine}$); 116.8 (*Ar*); 117.7 ($Ar_{acridine}$); 121.8 ($Ar_{acridine}$); 124.6 ($Ar_{acridine}$); 126.5 ($Ar_{acridine}$); 130.9 ($Ar_{acridine}$); 135.8 (*Ar*); 136.4 ($Ar_{acridine}$), 136.7 ($Ar_{acridine}$), 148.1 (*Ar*); 150.8 ($Ar_{acridine}$); 152.4-153.1 ($Ar_{acridine}$); 155.6 ($Ar_{acridine}$); 157.0 ($Ar_{acridine}$); 169.2 (H*C*=N). FT-IR (ATR): ν(cm^{-1}) = 3277 (N-H); 1629 (C=N)$_{imine}$, 1604 (C=N)$_{acr.\ imine}$, 1600 (C=N)$_{pyridylimine}$.. HR-ESI-MS (+): Calc. for $C_{32}H_{33}Cl_2N_4OOs$ $[M]^+$ *m/z* = 751.1646 Found: *m/z* = 1071.3418 $[(M+H)^{2+}BPh_4^-]^+$, *m/z* = 751.1634 $[M]^+$.

2.13 | X-ray crystallography

Single crystals of **C6** were obtained by slow diffusion of *n*-heptane (3 mL) into a concentrated solution of **C6** (0.005 g) in chloroform (2 ml) at room temperature. Crystal data

and collection details for **C6** are reported in Table 1. Single-crystal X-ray diffraction data were collected on a Bruker KAPPA APEX II DUO diffractometer using graphite-monochromated Mo-Kα radiation (χ = 0.71073 Å). Data collection was carried out at 173(2) K. Temperature was controlled by an Oxford Cryostream cooling system (Oxford Cryostat). Cell refinement and data reduction were performed using the program SAINT.[38] The data were scaled and absorption correction performed using SADABS.[39]

The structure was solved by direct methods using SHELXS-97[39] and refined by full-matrix least-squares methods based on F^2 using SHELXL-2014[39] and using the graphics interface program X-Seed.[40] The programs X-Seed and POV-Ray[41] were both used to prepare molecular graphic images.

TABLE 1 Crystallographic data for complex **C6**

	C6· (C_5 + O)
Empirical formula	$C_{61}H_{54}BCl_2N_4O_2Rh$
Formula weight	1059.70
Temperature/K	173(2)
Crystal system	triclinic
Space group	P-1
Crystal size	
0.130 x 0.100 x 0.050	
a/Å	12.9383(10)
b/Å	13.0568(11))
c/Å	16.1005(13)
α/°	85.570(2)
β/°	83.655(2)
γ/°	87.686(2)
Volume/$Å^3$	2693.8(4)
Z	2
μ (mm^{-1})	0.463
$\rho_{calc}g/cm^3$	1.306
F(000)	1096.0
Radiation	MoKα (λ = 0.71073)
Theta range for data collection/°	1.95< θ < 28.45
Reflections collected	70736
Unique reflections	13606
R_{int}	0.041
Data/restraints/parameters	13552/0/ 625
Goodness-of-fit on F^2	1.050
Final R indices [I > = 2σ (I)]	R_1 = 0.0417, wR_2 = 0.1119
Final R indices [all data]	R_1 = 0.0544, wR_2 = 0.1205
Max, Min Δρ/e/ $Å^{-3}$	1.26, -0.66

All non-hydrogen atoms, except those of *n*-heptane solvent molecule, were refined anisotropically. Only five out of seven carbon atoms in *n*-heptane could be positioned in the Fourier maps and were refined isotropically, the other two carbon atoms and all *n*-heptane's hydrogen atoms were excluded from the final model. The hydrogen atoms on the water molecule could not be located and were also excluded from the final model. All other hydrogen atoms, except the amino hydrogen atom H3N, were placed in idealized positions and refined in riding models with U_{iso} assigned 1.2 or 1.5 times U_{eq} of their parent atoms and the bond distances were constrained between 0.95 – 0.99 Å. The hydrogen atom H3N was located in the difference electron density maps and refined freely. The structure was refined to R factor of 0.0417. The parameters for crystal data collection and structure refinements, the bond lengths, angles, torsion angles are contained in file ac20.SUP.

CCDC number 1512942 contains the supplementary crystallographic data for complex **C6**. This data can be obtained free of charge from The Cambridge Crystallographic Data Centre. Copies of this information may be obtained free of charge from The Director, CCDC, 12 Union Road, Cambridge, CB2 1EZ, UK (fax: +44-1223/336-033; email: deposit@ccdc.cam.ac.uk or http://www.ccdc.cam.ac.uk/conts/retrieving.html.

2.14 | Cell culture

Human promyelocytic leukemia cells (HL60) and skin fibroblast cells (FG0) were maintained in RPMI-1640 medium (Gibco, Paisley, UK) and DMEM medium (Gibco, Paisley, UK) respectively. All media were supplemented with 10 % fetal bovine serum (FBS) and antibiotics (100 U/ml penicillin and 100 μg/ml streptomycin) and cells were cultured at 37°C in a 5 % CO_2 – 95% air-humidified incubator.

2.15 | Cytotoxicity assay

The compounds (**L1-L3, C1-C9** and **cisplatin**) were prepared as DMSO solutions then immediately dissolved in the culture medium and serially diluted to the appropriate concentration, to give a final DMSO concentration of 0.5%. For each compound, cells were seeded in 96 well plates at 1.0×10^4 cells per well and were prepared for treatment as follows: FG0 were cultured to 50-60% adherent confluency and were then treated by replacing normal culture media with treatment media containing compound or vehicle; whereas HL60 were grown in suspension for 24 hours and treatment media were added directly to the normal culture media already in wells to the desired final concentration. Cells were thus treated in quadruplicate with a range of concentrations of compound or vehicle for 48 hours while incubating at 37°C and 5 % CO_2. Cytotoxicity of the compounds was

evaluated using the 3-(4,5-dimethylthiazol-2-yl)-2,5-diphenyltetrazolium bromide (MTT) assay as per manufacturer's instructions (Roche, Indianapolis, Indiana USA). Briefly, 10 µl of MTT solution was added to each well and incubated at 37°C for 4 h. This was followed by addition of 100 µl solubilization buffer (10 % SDS in 0.01 *M* HCl) and incubation overnight at 37°C. Absorbance (585 nm) was then determined for each well and the mean cell viability was calculated as a percentage of the mean vehicle control. Each compound was assayed in triplicate (biological repeats) and the half maximal cytotoxic concentration values (IC_{50}) determined.

2.16 | Aqueous media and DMSO stability studies

Complex **C2** was dissolved in DMSO-d_6 / D_2O, in a 50:50 ratio (0.5 ml each), and warmed at 37°C, to mimic physiological conditions. The sample was monitored by ^{1}H NMR spectroscopy for stability at varying times up to 24 hours. In another experiment, **C2** was dissolved in DMSO-d_6 and 0.1 *M* NaCl (prepared using D_2O) (50:50 ratio, 0.5 ml each), and the sample was monitored by ^{1}H NMR spectroscopy for stability at varying times up to 24 hours.

2.17 | 5'-GMP model DNA interactions studies

C2, and an equimolar amount of 5'-GMP were dissolved in DMSO-d_6 / D_2O, in a 50:50 ratio (0.5 ml each) and warmed at 37°C, to mimic physiological conditions. The sample was monitored by ^{1}H NMR and ^{31}P{^{1}H} NMR spectroscopy at varying times up to 24 hours. In another experiment, **C2** and an equimolar amount of 5'-GMP were dissolved in DMSO-d_6 and 0.1 *M* NaCl (prepared using D_2O) (50:50 ratio, 0.5 ml each), and the sample was monitored by ^{1}H NMR and ^{31}P{^{1}H} NMR spectroscopy at varying times up to 24 hours.

3 | RESULTS AND DISCUSSION

3.1 | Synthesis and characterization of acridine ligands (L1 –L3 and C1)

N^1-(6-chloro-2-methoxyacridin-9-yl)ethane-1,2-diamine (**L1**) was synthesized using the procedure described by Tot *et al.*[37] 6,9-Dichloro-2-methoxyacridine was added to excess ethylene diamine and refluxed for 20 hours (Scheme 1). **L1** was isolated in 75% yield as an orange solid. Acridinyl imine ligands **L2** and **L3** were prepared by a Schiff-base condensation reaction of **L1** with salicylaldehyde and 2-pyridine carboxaldehyde in dichloromenthane at room temperature (Scheme 1). The ligands (**L2** and **L3**) were obtained as air- and moisture-stable orange solids in good

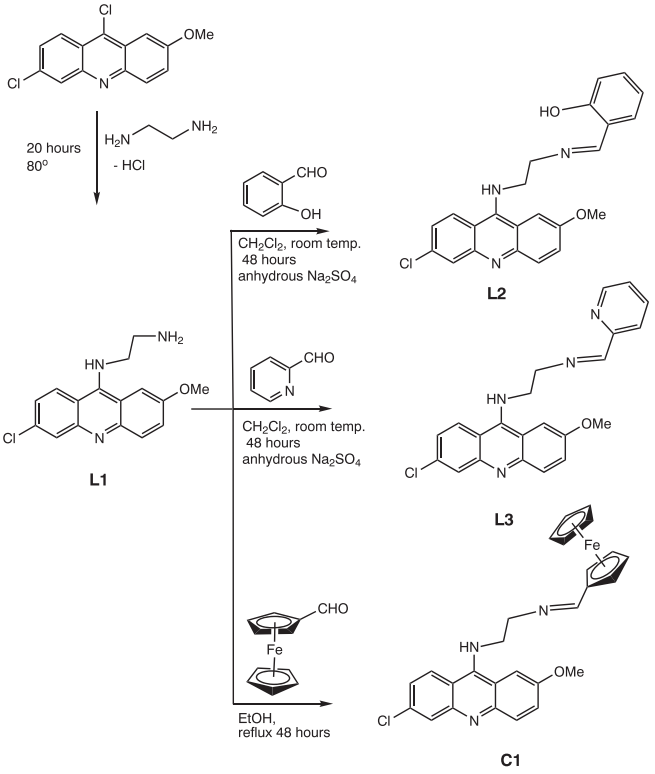

SCHEME 1 Outline for the synthesis of amino- and imino-acridine ligands (**L1**-**L3**) and ferrocenyl-acridine complex **C1**

yields of 72 and 75 % respectively and were fully characterized using analytical and spectroscopic techniques.

The ^{1}H NMR spectra for ligands **L2** and **L3** all display characteristic imine singlets in the range of δ = 8.09 to 8.26. The acridinyl and phenyl aromatic protons for **L2** and **L3** are observed in the range of δ = 6.82 to 8.37 and δ = 7.18 to 8.45 respectively. In the aliphatic region, signals due to the CH_2 groups of the ethylene linker (integrating for 2 protons each) and the methoxy (OMe) groups are seen in the region of δ = 3.71 to 4.05. In addition, the spectrum for **L2** shows a signal due to the phenolic proton at δ = 12.90. In the ^{13}C NMR spectra for **L2** and **L3**, the aliphatic carbons are observed between δ = 49.9 and δ = 61.1 and the aromatic carbons between δ = 97.7 and 160.5. The chemical shifts for the signals of the imine carbons resonate at δ = 167.3 and 164.2 for ligands **L2** and **L3** respectively. FT-IR spectroscopy also confirms the formation of **L2** and **L3** by the presence of characteristic imine bands at 1630 cm^{-1} and 1647 cm^{-1} respectively. The acridinyl imine stretching vibration bands are displayed at *ca* 1600 cm^{-1} and amino (N-H) stretching vibration bands are evident at *ca* 3350 cm^{-1}. Further evidence for the formation of **L2** and **L3** is shown by high resolution ESI-mass spectrometry results, which exhibit peaks assigned to $[M+H]^+$ ions at *m/z* = 406.1240 and *m/z* = 391. 1253.

The ferrocenyl acridine-containing complex **C1** was obtained *via* a Schiff-base condensation of **L1** with a slight

excess of ferrocene carboxaldehyde (Scheme 1) in ethanol. **C1** precipitated and was collected by filtration as an orange solid in a yield of 39%. This compound is soluble in most organic solvents except petroleum ether, *n*-hexane and *n*-heptane. The ^{1}H NMR spectrum of **C1** displays a characteristic imine signal at δ = 8.13, confirming the formation of **C1**. Broad signals at δ = 4.50 and δ = 4.33 represent the protons on the substituted cyclopentadienyl (Cp) ring. The broad signal integrating for 10 protons seen at δ = 3.90 to 4.04 is assigned to the methoxy group (OMe), the one CH_2 group and the protons on the unsubstituted Cp ring. An imine signal at δ = 162.5 is observed in the ^{13}C NMR spectrum of **C1** while other carbon signals are consistent with the proposed structure.

In the FT-IR spectrum of **C1**, the acridinyl imine absorption band appears at 1606 cm^{-1} while the imine band is seen at 1630 cm^{-1}. An N-H stretching vibration band is also observed at 3425 cm^{-1}. The mass spectrum displays a *m/z* = 498.1036 peak corresponding to $[M+H]^+$, (Figure S1) thus further confirming the formation of **C1**.

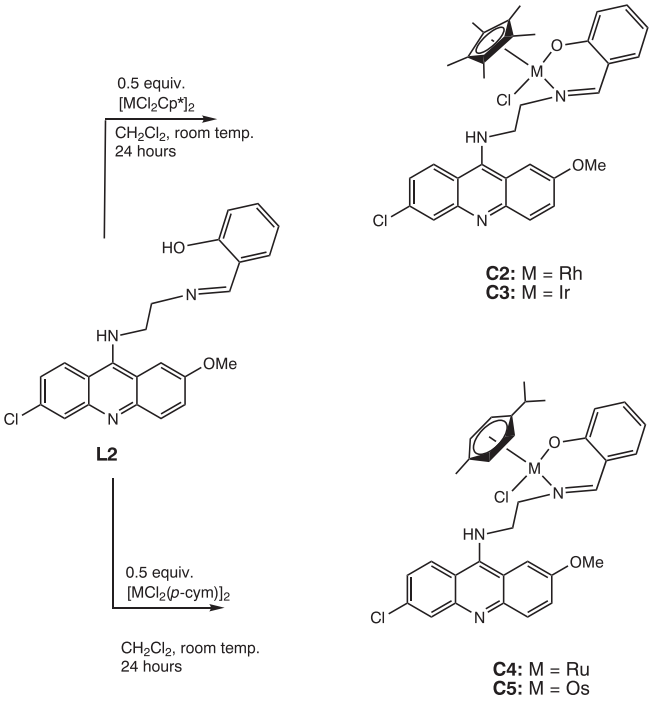

SCHEME 2 Outline of the synthesis of neutral acridine-containing complexes (**C2**-**C5**)

3.2 | Synthesis and characterization of acridine-containing neutral complexes (C2 –C5)

The acridine–containing complexes (**C2**-**C5**) were obtained by reacting a deprotonated **L2** in dichloromethane with dimeric precursors, $[Ru(p\text{-cym})Cl_2]_2$, $[Os(p\text{-cym})Cl_2]_2$, $[RhCp^*Cl_2]_2$, and $[IrCp^*Cl_2]_2$ (where *p*-cym = η^6-*p*-^{i}PrC$_6$H$_4$Me and Cp* = η^5-C$_5$Me$_5$) at room temperature over 24 hours (Scheme 2). These new complexes were obtained as yellow to orange air- and moisture-stable solids in good yields ranging from 58-99%.

Upon complexation of the metals to the acridinyl salicylaldiminato ligand (**L2**) a distinct shift of the imine proton signals (from δ = 8.26 in **L2** to δ = 7.98, 8.04, 7.92 and 7.90 in **C2**, **C3**, **C4** and **C5** respectively) is seen in the ^{1}H NMR spectra of the complexes. This confirms coordination of the metals at the imine nitrogen. There is no evidence of coordination at the acridinyl nitrogen in all the complexes. The pentamethylcyclopentadienyl (Cp*) protons of the Rh(III) and Ir(III) complexes (**C2** and **C3**) are observed as singlets in the range of δ = 1.49 to 1.64 and are similar to what has been previously reported.[19, 42] For the Ru(II) and Os(II) complexes (**C4** and **C5**), the *p*-cym ligands exhibit expected ^{1}H NMR signals. Two chemical shifts for the methyl protons are seen at δ = 1.02 to 1.17 (assigned to the isopropyl methyl groups) and at *ca* δ = 2.1 (for the methyl groups directly bonded to the arene ring). The aromatic protons of the *p*-cym resonate as multiplets between δ = 5.36 to 6.15 due to metal center induced chirality.[18,42–45] This metal center induced chirality also imparts splitting of the proton signals assigned to the CH_2 functionalities adjacent to the imine nitrogens (from one signal in the spectrum for **L2**) to two diastereotopic proton signals in the spectra of complexes **C2**-**C5**. For example, in **C2** this CH_2 group gives rise to two distinct signals comprising broad singlets at δ = 4.18, and δ = 4.33. All other aromatic protons for the salicylaldimine and acridine moieties (and its substituents) were observed in the expected regions. The ^{13}C NMR spectra display the most deshielded carbons in the range of δ = 165.8 to 166.3 assigned to the imine carbons of complexes **C2 – C5**. These have shifted from δ = 167.3 in **L2** further confirming coordination of the metal centers to the imine nitrogen.

^{13}C NMR spectra of the complexes (**C2**-**C5**) also display signals in the region of δ = 9.06 to 69.9 assigned to the aliphatic carbons. Overall, complexes **C2**-**C5** display chemical shifts for aromatic carbons in the range of δ = 76.4 to 164.4, inclusive of the signals due to the respective co-ligands (Cp* and *p*-cym).

Further analysis by FT-IR shows expected N-H stretch vibration bands in their characteristic region of 3309 to 3321 cm^{-1} for **C2**-**C5**, and the $\nu(C{=}N)_{imine}$ stretching bands have shifted to lower absorption frequencies upon complexation. The $(C{=}N)_{imine}$ bond experiences electron-withdrawing effects from the aromatic ring and the coordinated metals which weakens the bond, resulting in a shift to lower frequencies. Additionally, the absence of the ν(OH) stretching vibration band gives confirmation of coordination in a bidentate N^O manner and that **L2** acts as anionic bidentate donor ligand. When analyzed by high resolution

mass spectrometry, these complexes all display peaks corresponding to the $[M+H]^+$ and $[M-Cl]^+$ ions.

3.3 | Synthesis and characterization of acridine-containing cationic complexes (C6 – C9)

The N^N donor ligand (**L3**) was reacted with 0.5 equivalents of the appropriate metal precursors, $[Ru(p\text{-cym})Cl_2]_2$, $[Os(p\text{-cym})Cl_2]_2$, $[RhCp^*Cl_2]_2$, and $[IrCp^*Cl_2]_2$ in chloroform (Scheme 3). The ruthenium and osmium analogues are unstable if left to stir for longer than 90 minutes, after which decomposition to a black solution is observed.

The acridine-containing 2-pyridylimine ligand (**L3**) bonds to the metal centers in a bidentate manner *via* the pyridyl and imine nitrogen atoms to produce cationic complexes. These complexes were further treated with sodium tetraphenyl borate ($Na[BPh_4]$) in an anion metathesis reaction to ensure air-stability,[18,23b] thus yielding new complexes (**C6**-**C9**). The complexes were obtained in yields ranging from 61 to 72% and are all soluble in warm water (± 40°C) and in organic solvents such as acetonitrile, acetone, chloroform, ethanol and dichloromethane.

^{1}H NMR spectroscopy confirmed coordination of the metal centers to both the pyridylimine and imine nitrogen atoms. A notable feature includes a downfield shift in the imine proton signal from δ = 8.42 in **L3** to *ca* δ = 8.3 in the complexes. There is also a characteristic downfield shift in the signals for the proton adjacent to the pyridyl nitrogen for all complexes (**C7**-**C9**) due to the coordination of the Ru(II), Os(II), Rh(III) and Ir(III) ions. The coordination induces diastereotopicity in these complexes as well, and this is evidenced by splitting of the proton signals assigned to the CH_2 group directly bonded to the imine nitrogens. This signal is seen as broad singlets at δ = 4.45 and δ = 4.54 in **C6**. There are no significant shifts in the acridinyl proton signals (and its substituent OMe) and this observation implies that no metal coordination occurs at the acridinyl imine. All other aromatic protons for the 2-pyridylimine, Cp* and *p*-cym moieties were observed in the expected regions in the ^{1}H NMR spectra of complexes **C6**-**C9**.

^{13}C NMR spectra for **C6**-**C9** all show the expected number of signals for the proposed structures, with the imine carbon signals shifting slightly downfield to δ = 169.7 (**C6**), δ = 171.1 (**C7**), δ = 170.4 (**C8**) and δ = 169.2 (**C9**), from δ = 164.2 in **L3**. The methyl substituents on the Cp* ligand resonate between δ = 7.7 and 8.6 while the remaining carbons of the Cp* ring are seen at δ = 89.4 and 97.5 for **C7** and **C6** respectively. The *p*-cym ligands in **C8** and **C9** display aromatic signals in the range of δ = 84.6 to 102.2.

The infrared spectra of complexes (**C6**-**C9**) show the $(C{=}N)_{imine}$ stretching frequency band at lower wavenumbers of *ca* 1630 cm^{-1} from 1647 cm^{-1} in **L3** while the absorption bands assigned to the $(C{=}N)_{pyridylimine}$ stretching frequencies experience slight shifts to higher wavenumbers of *ca* 1600 cm^{-1} from 1597 cm^{-1} in **L3**. The former is as a result of the pyridyl functional groups and the

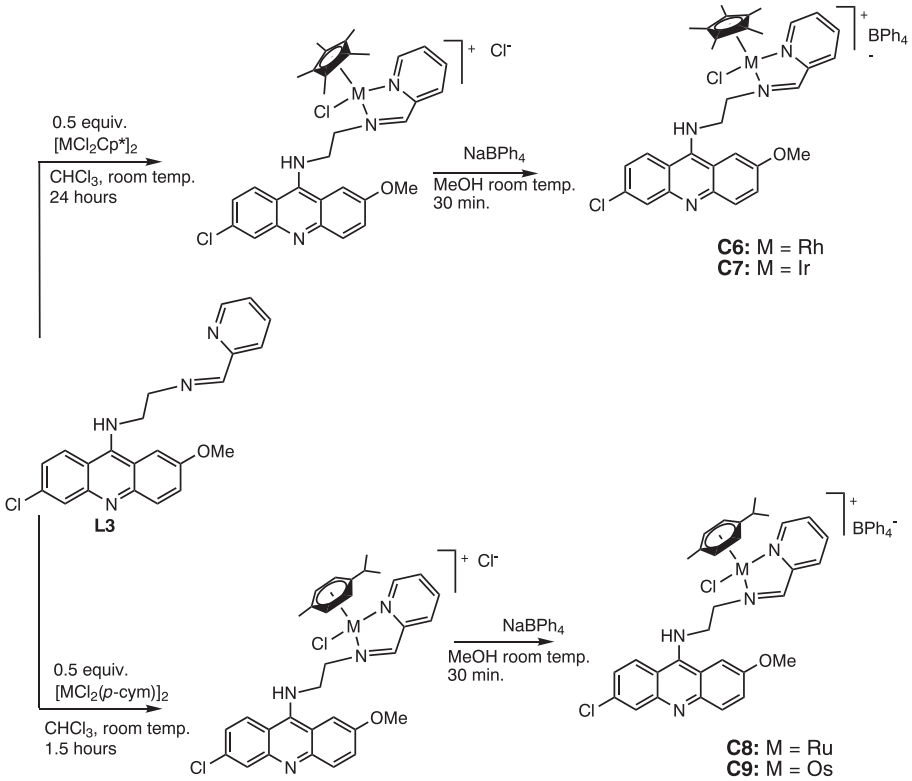

SCHEME 3 Outline of the synthesis cationic acridine-containing complexes (**C6**-**C9**)

coordinated metal centers effectively withdrawing electrons from to the $(C=N)_{imine}$ bond thereby causing a shift to lower wavenumbers.

HR-ESI mass spectrometry was used for further characterization of the complexes and is consistent with the formation of **C6-C9** by displaying $[(M+H)^{2+}BPh_4^-]^+$ ion peaks. Interestingly, though conducted in the positive mode for all the complexes, the metal salt plus H^+ ion $[(M+H)^{2+}BPh_4^-]^+$ was detected.[50] This may be attributed to the fact that electron spray is a soft ionization technique and that the analyses were conducted at a low 15V.

3.4 | X-ray diffraction studies of complex C6

The molecular structure of complex (**C6**) was unambiguously confirmed in the solid state by single crystal X-ray diffraction. Orange single crystals suitable for X-ray diffraction were obtained by slow diffusion of *n*-heptane into a concentrated solution of **C6** in chloroform at room temperature. The molecular structure of **C6** is depicted in (Figure 3) together with geometric parameters. Further crystallographic details are given in Table 1.

Complex **C6** crystalizes in the triclinic crystal system and P_{-1} space group. The molecular structure of (**C6**) shows a typical piano-stool geometry with the rhodium center coordinated to the Cp* ligand in an *eta*-(5)-fashion. Other ligands around the rhodium include a terminal chloride and a chelating N^N ligand.

The Rh-N bond distances range from 2.118(2) Å to 2.116(2) Å in **C6** and are comparable to those in similar N^N Rh(III) complexes.[42,46] Accordingly, there is no significant differences in the Rh-Cl bond lengths of **C6** (2.3861(7) Å as compared to reported values.[19,42]

TABLE 2 *In vitro* IC_{50} values of compounds **L1-L3** and **C1-C9** determined against the human promyelocytic leukemia (HL60) cancer cell line and FG0 (normal skin fibroblast) cells, by MTT assay

Compound	HL60 IC_{50} [μM] ± SD[a]	FG0 IC_{50} [μM] ± SD [a]	SI (FG0/HL60)
L1	2.50 ± 0.66	5.85 ± 1.70	2.34
L2	2.49 ± 0.50	10.02 ± 0.18	4.02
L3	3.76 ± 0.13	7.14 ± 0.60	1.89
C1	2.82 ± 0.01	22.64 ± 3.00	7.94
C2	1.97 ± 0.14	6.50 ± 0.14	3.29
C3	2.34 ± 0.80	5.72 ± 1.90	2.44
C4	2.89 ± 0.18	7.38 ± 0.90	2.55
C5	10.20 ± 0.03	27.80 ± 1.70	2.72
C6	2.51 ± 1.30	3.00 ± 0.01	1.19
C7	3.48 ± 0.01	12.74 ± 0.70	3.28
C8	6.20 ± 0.20	34.35 ± 1.30	5.54
C9	9.16 ± 0.16	29.10 ± 0.30	3.17
cisplatin	6.57 ± 0.11	42.13 ± 1.90	6.41

[a]50% inhibitory concentrations as obtained by the MTT assay and the values are means ± standard deviations obtained from at least three independent experiments. SI is the selectivity index determined as a ratio of the IC_{50} value of the FG0 cells over the IC_{50} value of HL60 cells.

3.5 | *In Vitro* anticancer activity of compounds L1-L3 and C1-C9

The antiproliferative activity of the ligands (**L1-L3**) and complexes (**C1-C9**) were evaluated *in vitro* against the human promyelocytic leukemia cell line (HL60) and a non-cancerous skin fibroblast cell line (FG0). The IC_{50} values obtained as an average of three independent determinations are shown in Table 2.

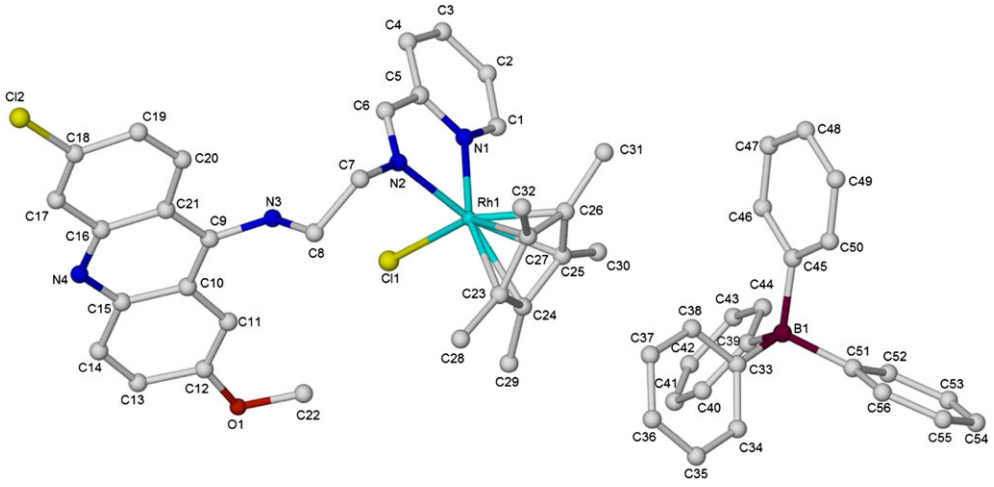

FIGURE 3 The ORTEP drawing of the molecular structure of complex (**C6**), showing atomic labelling. Ellipsoids are at 40 % probability level, hydrogens omitted for clarity. Selected bond distances (Å) and angles (°): Rh(1)-N(1), 2.118(2); Rh(1)-N(2), 2.116(2); Rh(1)-Cl(1), 2.3861(7); Cl(1)-Rh(1)-N(1), 85.71(6); Cl(1)-Rh(1)-N2(1), 88.14(6); N(1)-Rh(1)-N(2), 76.63(8)

All the compounds display higher cytotoxicities when compared to cisplatin for the HL60 cell line apart from Os(II) complexes **C5** and **C9** which had low solubility in the cell culture medium, and this may have resulted in decreased uptake into the cells. The ligands (**L1-L3**) display good activities and upon coordination to Rh(III) and Ir(III) (**C2**, **C3**, **C6** and **C7**), an increase in antiproliferative activity is demonstrated. The Fe(II), Ru(II) and Os(II) complexes (**C1**, **C4**, **C5**, **C8** and **C9**), all exhibit slightly lower activities in comparison to the Rh(III) and Ir(III) complexes (**C2**, **C3** and **C6**).

In general, the neutral complexes (**C2-C4**) exhibit better activity than their cationic (**C6-C8**) congeners except for osmium complexes **C5** and **C9**, where the cationic complex is slightly more cytotoxic than the neutral complex. The IC_{50} values of the ligands and complexes are comparable to a previously reported platinum complex conjugated with an acridine moiety (against HL60 cells) although the cytotoxic measurements were not conducted using the same assay.[27b]

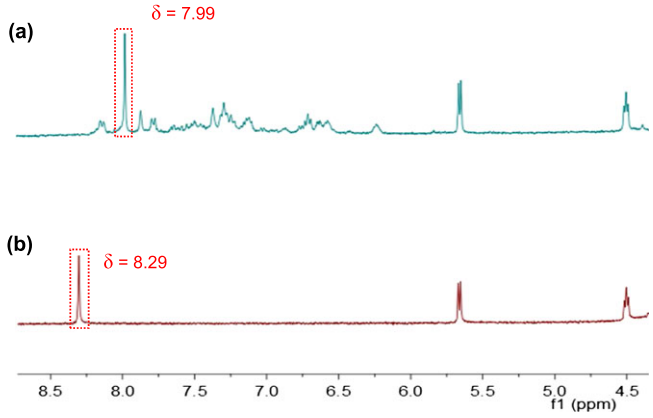

FIGURE 4 (a) ^{1}H NMR spectrum of the reaction mixture of **C2** and 5'-GMP in DMSO-d_6/D_2O (50:50 *v/v*) and (b) ^{1}H NMR spectrum of the 5'-GMP in DMSO-d_6/D_2O (50:50 *v/v*). Spectra were recorded after incubation at 37 °C for 2 hours

Importantly, all the compounds proved to be consistently selective towards the cancer cell line over the normal FG0 cells with **C6** being the least selective towards cancer cells (selectivity index, SI = 1.19).

3.6 | Stability and 5'-GMP binding NMR studies

An accepted mode of action of metal complexes under physiological conditions involves the substitution of a chloride ligand with a solvent molecule to form a metal-aqua species which subsequently interacts with DNA base pairs.[47] NMR studies were employed to assess the stability of complex **C2** (which displayed the best cytotoxicity) in DMSO-d_6/D_2O (50:50 *v/v*) over 24 hours at 37°C. This solvent solution was used to mimic the preparation solution prior to conducting the biological assays. In addition, the same experiments were conducted with **C2** using 0.1 *M* NaCl solution in D_2O/DMSO-d_6 (50:50 *v/v*) (instead of plain D_2O) in order to mimic a chloride concentration similar to that present in the blood. Complex **C2** proved to be stable in both solutions over 24 hours and there are no signs of aquation or any side product formation (Figure S8).[50]

The binding of metal complexes to DNA and/or proteins is a significant step in the cytotoxic mechanism of metal-based drugs, and studies have shown that metal complexes preferentially bind to guanine.[48,49] Thus, interaction of **C2** with DNA model guanosine-5'-monophosphate (5'-GMP) was monitored by ^{1}H and ^{31}P{^{1}H} NMR spectroscopy in both DMSO-d_6/D_2O (50:50 *v/v*) and 0.1 *M* NaCl in D_2O/DMSO-d_6 (50:50 *v/v*) solutions. NMR measurements were taken after incubation for two hours, where complex **C2** is seen to interact with the DNA model, 5'-GMP, by complexing to its N7 atom. This is evidenced by an upfield shift of the proton signal on the carbon (C8) adjacent to N7

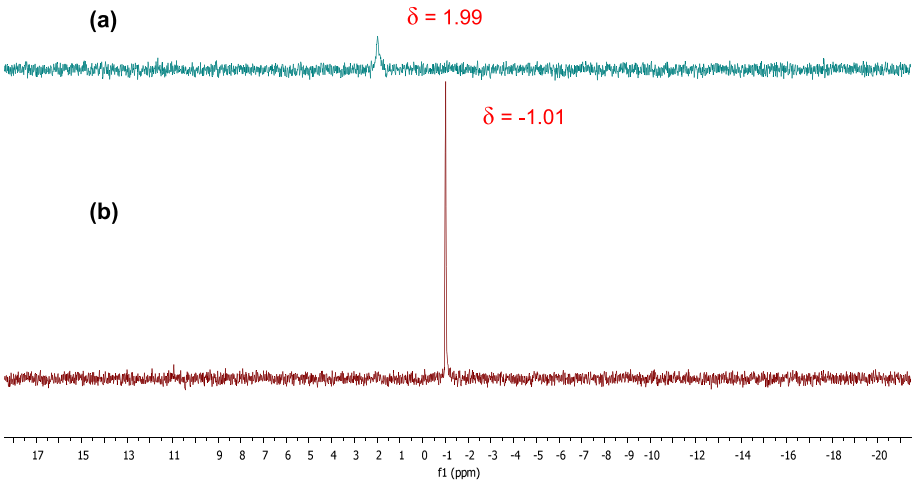

FIGURE 5 31P{1H} NMR spectrum of (a) 5'-GMP DMSO-d6/D2O (50:50 *v*/v) and (b) ^{31}P{^{1}H} NMR spectrum of **C2** and 5'-GMP in DMSO-d_6/D_2O (50:50 *v/v*). Spectra were recorded after incubation at 37°C for 2 hours

from $\delta = 8.29$ (for free 5-GMP, Figure 4b) to $\delta = 7.99$ (in the adduct, Figure 4a). The high stability in solution demonstrated by **C2**, suggest that 5'-GMP binding occurs *via* a direct chloride ligand substitution on the metal center. Additionally, the $^{31}P\{^{1}H\}$ spectra of the free 5'-GMP and the mixtures show an upfield shift in the phosphorus (monophosphate) signal from $\delta = 1.99$ (in free 5'-GMP) to $\delta = -1.01$ in the adduct (Figure 5(a) and 5(b)). This suggests that acridine is likely playing the role of a vector, directing the complex to the DNA. The cytotoxic mechanism may involve a dual action where DNA intercalation is driven by the acridine scaffold, and further metal complex interaction with the DNA base pairs. More specifically, binding to 5'-GMP nucleotide found in the DNA backbone is a possible mode of action for such systems.

4 | CONCLUSIONS

New acridine-containing salicylaldimine and 2-pyridylimine ligands, ferrocenyl and half-sandwich Rh(III), Ir(III), Ru(II) and Os(II) complexes have been successfully prepared and characterized using an array of spectroscopic and analytical techniques. The molecular structure of the cationic Rh(III) complex, **C6**, has been determined by single crystal X-ray diffraction. All the compounds display good *in vitro* cytotoxicities against the human promyelocytic leukemia cell line. The coordination of metal cations to the acridine-containing ligands results in slightly improved activity against HL60, apart from the Os(II) ion. Neutral N^O chelating complexes (**C2-C5**) exhibit better antiproliferative activities over the cationic systems, and there is a notable selectivity towards cancer cells (HL60) in comparison to normal skin fibroblast cells (FG0). NMR studies show that the most active complex (**C2**) is stable in aqueous solution (including NaCl aqueous solution) and that this complex binds to 5'-GMP, thus suggesting that DNA is an *in vitro* target.

ACKNOWLEDGMENTS

We would like to thank the University of Johannesburg, the University of Cape Town the National Research Foundation of South Africa (NRF) (Grant Number 95517) for financial support.

REFERENCES

[1] http://www.who.int/mediacentre/factsheets/fs297/en/ (accessed 13 March 2015).

[2] https://www.cancer.org/acs/groups/content/@nho/documents/document/globalfactsandfigures2007rev2p.pdf American Cancer Society, Global Cancer – Facts & Figures 2007, p. 1, (accessed 23 January 2014.)

[3] B. Rosenberg, L. Van Camp, J. E. Trosko, V. H. Mansour, *Nature* **1969**, *222*, 385.

[4] www.accessdata.fda.gov/drugsatfda_docs/label/2011/018057s080lbl.pdf US Food and Drug Administration, (accessed 26 April 2014).

[5] M. Galanski, V. B. Arion, M. A. Jakupec, B. K. Keppler, *Curr. Pharm. Des.* **2003**, *9*, 2078.

[6] M. A. Jakupec, M. Galanski, B. K. Keppler, *Rev. Physiol. Biochem. Pharmacol.* **2003**, *146*, 1.

[7] M. Galanski, M. A. Jakupec, B. K. Keppler, *Curr. Med. Chem.* **2005**, *12*, 2075.

[8] M. J. Clarke, *Coord. Chem. Rev.* **2003**, *236*, 209.

[9] M. J. Clarke, F. Zhu, D. R. Frasca, *Chem. Rev.* **1999**, *99*, 2511.

[10] M. A. Jakupec, B. K. Keppler in: A. Sigel, H. Sigel (Eds.), *Metal Ions in Biological Systems*, vol. 42, Dekker, New York, **2004**, 425.

[11] E. Wong, C. M. Giandomenico, *Chem. Rev.* **1999**, *99*, 2451.

[12] K. Wu, Q. Luo, W. Hu, X. Li, F. Wang, S. Xiong, P. J. Sadler, *Metallomics* **2012**, *4*, 139.

[13] (a) J. Maksomiska, D. S. Williams, G. E. Atilla-Gokcumen, K. S. M. Smalley, P. J. Carroll, R. D. Webster, P. Filippakopoulos, S. Knapp, M. Herlyn, E. Meggers, *Chem.–Eur. J.* **2008**, *14*, 4816; (b) P. Govender, L. C. Sudding, C. M. Clavel, P. J. Dyson, B. Therrien, G. S. Smith, *Dalton Trans.* **2013**, *42*, 1267.

[14] (a) P. J. Dyson, G. Sava, *Dalton Trans.* **2006**, *16*, 1929; (b) C. Scolaro, A. Bergamo, L. Brescacin, R. Delfino, M. Cocchietto, G. Laureneczy, T. J. Geldbach, G. Sava, P. J. Dyson, *J. Med. Chem.* **2005**, *48*, 4161.

[15] P. Govender, A. K. Renfrew, C. M. Clavel, P. J. Dyson, B. Therrien, G. S. Smith, *Dalton Trans.* **2011**, *40*, 1158.

[16] A. A. Nazarov, C. G. Hartinger, P. J. Dyson, *J. Organomet. Chem.* **2014**, *751*, 251.

[17] P. Govender, T. Riedel, P. J. Dyson, G. S. Smith, *J. Organomet. Chem.* **2015**, *799-800*, 38.

[18] (a) B. C. E. Makhubela, M. Meyer, G. S. Smith, *J. Organomet. Chem.* **2014**, *772*, 229; (b) P. Govender, F. Edafe, B. C. E. Makhubela, P. J. Dyson, B. Therrien, G. S. Smith, *Inorg. Chim. Acta* **2014**, *409*, 112.

[19] (a) A. R. Burgoyne, B. C. E. Makhubela, M. Meyer, G. S. Smith, *Eur. J. Inorg. Chem.* **2015**, 1433; (b) A. Wilbuer, D. H. Vlecken, D. J. Schmitz, K. Kräling, K. Harms, C. P. Bagowski, E. Meggers, *Angew. Chem. Int. Ed.* **2010**, *49*, 3839; (c) J. Ruiz, V. Rodriguez, N. Cutillas, K. G. Samper, M. Capdevila, O. Palacios, A. Espinosa, *Dalton Trans.* **2012**, *41*, 12847.

[20] S. H. van Rijt, A. F. A. Peacock, R. D. L. Johnstone, S. Parsons, P. J. Sadler, *Inorg. Chem.* **2009**, *48*, 1753.

[21] P. Heffeter, B. Atil, K. Kryeziu, D. Groza, G. Koellensperger, W. Korner, U. Jungwirth, T. Mohr, B. K. Keppler, W. Berger, *Eur. J. Cancer* **2013**, *49*, 3366.

[22] A. Bergamo, G. Sava, *Dalton Trans.* **2007**, *13*, 1267.

[23] (a) G. Agonigi, T. Riedel, M. Gay, L. Biancalana, E. Oñate, P. J. Dyson, G. Pampaloni, E. Păunescu, M. A. Esteruelas, F. Marchetti, *Organometallics* **2016**, *35*, 1046; (b) N. Wambang, N. Scifano-Faux, A. Martoriati, N. Henry, B. Baldeyrou, C. Bal-Mahieu, T. Bousquet, S. Pellegrini, S. Meihnan, K. Cailliau, J.-F. Goossens,

J.-F. Bodart, P. T. Ndifon, L. Pélinksi, *Organometallics* **2016**, *35*, 2668.

[24] R. Guddneppanavar, J. R. Choudhury, A. R. Kheradi, B. D. Steen, G. Saluta, G. L. Kucera, C. S. Day, U. Bierbach, *J. Med. Chem.* **2007**, *50*, 2259.

[25] (a) R. V. Chari, M. L. Miller, W. C. Widdison, *Angew. Chem. Int. Ed.* **2014**, *53*, 3796; (b) R. Pettinari, F. Marchetti, A. Petrini, C. Pettinari, G. Lupidi, P. Smoleński, R. Scopelliti, T. Riedel, P. J. Dyson, *Organometallics* **2016**, *35*, 3734.

[26] (a) W. Wang, W. C. Ho, D. T. Dicker, C. Mackinnon, J. D. Winkler, R. Marmorstein, W. S. El-deiry, *Cancer Biol. Ther.* **2005**, 893; (b) M. A. Horstmann, W.-A. Hassenpflug, *Hematol. J.* **2005**, *90*, 1701; (c) K. Gorlewska, Z. Mazerska, P. Sowinski, J. Konopa, *Chem. Res. Toxicol.* **2001**, *14*, 1; (d) E. Augustin, A. Mość-Rompa, D. Nowak-Ziatyk, J. Konopa, *Biochem. Pharmacol.* **2010**, *79*, 1231.

[27] (a) C.-W. Ong, J.-Y. Jeng, S.-S. Juang, C.-F. Chen, *Bioorg. Med. Chem. Lett.* **1992**, *2*, 929; (b) E. T. Martins, H. Baruah, J. Kramarczyk, G. Saluta, C. S. Day, G. L. Kucera, U. Bierbach, *J. Med. Chem.* **2001**, *44*, 4492.

[28] H. Baruah, C. L. Rector, S. M. Monnier, U. Bierbach, *Biochem. Pharmacol.* **2002**, *64*, 191.

[29] Z. Ma, L. Rao, U. Bierbach, *J. Med. Chem.* **2009**, *52*, 3424.

[30] S. Ding, X. Qiao, G. L. Kucera, U. Bierbach, *Chem. Commun.* **2013**, *49*, 2415.

[31] H. W. Kava, A. M. Galea, F. M. Jamil, Y. Feng, V. Murray, *J. Biol. Inorg. Chem.* **2014**, *19*, 997.

[32] A. J. Pickard, F. Liu, T. F. Bartenstein, L. G. Haines, K. E. Levine, G. L. Kucera, U. Bierbach, *Chem.* **2014**, *20*, 16174.

[33] T.-S. A. Tseng, J. N. Burstyn, *Chem. Commun.* **2008**, 6209.

[34] M. A. Bennett, T. N. Huang, T. W. Matheson, A. K. Smith, *Inorg. Synth.* **1982**, *21*, 74.

[35] H. S. Clayton, B. C. E. Makhubela, H. Su, G. S. Smith, J. R. Moss, *Polyhedron* **2009**, *28*, 1511.

[36] C. White, A. Yates, P. M. Maitlis, *Inorg. Synth.* **1992**, *29*, 228.

[37] M. Tot, D. M. Opsenica, Ć. M. Mitrić, J. C. Burnett, L. Gomba, S. Bavari, B. A. Šolaja, *J. Serb. Chem. Soc.* **2013**, *78*, 131.

[38] SAINT Version 7.60a, Bruker AXS Inc., Madison, WI, USA, **2006**.

[39] G. M. Sheldrick, SHELXS-97, SHELXL-2014 and SADABS version 2.05, University of Göttingen, Germany, **1997**.

[40] (a) L. J. Barbour, *J. Supramol. Chem.* **2001**, *1*, 189; (b) J. L. Atwood, L. J. Barbour, *Cryst. Growth Des.* **2003**, *3*, 3.

[41] http://www.povray.org

[42] R. Payne, P. Govender, B. Therrien, C. M. Clavel, P. J. Dyson, G. S. Smith, *J. Organomet. Chem.* **2013**, *729*, 20.

[43] N. Komiya, T. Nakajima, M. Hotta, T. Maeda, T. Matsuoka, S. Kawamorita, T. Naota, *Eur. J. Inorg. Chem.* **2016**, 3148.

[44] L. C. Sudding, R. Payne, P. Govender, F. Edafe, C. M. Clavel, P. J. Dyson, B. Therrien, G. S. Smith, *Organomet. Chem.* **2014**, *774*, 79.

[45] B. C. E. Makhubela, A. M. Jardine, G. Westman, G. S. Smith, *Dalton Trans.* **2012**, *41*, 10715.

[46] G. Gupta, S. Gloria, S. L. Nongbr, B. Therrien, K. M. Rao, *J. Organomet. Chem.* **2011**, *696*, 2014.

[47] C. Gossens, A. Dorcier, P. J. Dyson, U. Rothlisberger, *Organometallics* **2007**, *20*, 3969.

[48] A. E. Egger, C. G. Hartinger, A. K. Renfrew, P. J. Dyson, *J. Biol. Inorg. Chem.* **2010**, *15*, 919.

[49] H. Chen, J. A. Parkinson, R. E. Morris, P. J. Sadler, *J. Am. Chem. Soc.* **2003**, *125*, 175.

[50] (a) Figure S1-S7 in the supporting information; (b) Figure S-8 in the supporting information.

SUPPORTING INFORMATION

Additional Supporting Information may be found online in the supporting information tab for this article.

How to cite this article: Matsheku AC, Chen MY-H, Jordaan S, Prince S, Smith GS, Makhubela BCE. Acridine-containing Ru^{II}, Os^{II}, Rh^{III} and Ir^{III} Half-Sandwich Complexes: Synthesis, Structure and Antiproliferative Activity. *Appl Organometal Chem*. 2017;e3852. https://doi.org/10.1002/aoc.3852